Journal of Theoretical Biology 303 (2012) 1–14

Contents lists available at SciVerse ScienceDirect

Journal of Theoretical Biology

journal homepage: www.elsevier.com/locate/yjtbi

Assessing the role of spatial heterogeneity and human movement in malaria dynamics and control

Olivia Prosper [a,*], Nick Ruktanonchai [b], Maia Martcheva [a]

[a] Department of Mathematics, University of Florida, Gainesville, FL, United States
[b] Department of Biology, University of Florida, Gainesville, FL, United States

ARTICLE INFO

Article history:
Received 30 April 2011
Received in revised form
7 February 2012
Accepted 8 February 2012
Available online 22 February 2012

Keywords:
Reproduction number
Elasticity analysis
Metapopulation model

ABSTRACT

Mathematical models developed for studying malaria dynamics often focus on a single, homogeneous population. However, human movement connects environments with potentially different malaria transmission characteristics. To address the role of human movement and spatial heterogeneity in malaria transmission and malaria control, we consider a simple malaria metapopulation model incorporating two regions, or patches, connected by human movement, with different degrees of malaria transmission in each patch. Using our two-patch model, we calculate and analyze the basic reproduction number, R_0, an epidemiologically important threshold quantity that indicates whether malaria will persist or go extinct in a population. Although R_0 depends on the rates of human movement, we show that R_0 is always bounded between the two quantities R_{01} and R_{02}—the reproduction numbers for the two patches if isolated. If without migration, the disease is endemic in one patch but not in the other, then the addition of human migration can cause the disease to persist in both patches. This result indicates that regions with low malaria transmission should have an interest in helping to control or eliminate malaria in regions with higher malaria endemicity if human movement connects them. Performing a sensitivity analysis of R_0 and the endemic equilibrium to various parameters in the two-patch model allowed us to determine, under different parameterizations of the model, which patch will be the better target for control measures, and within that patch, what type of control measure should be implemented. In the analysis of R_0, we found that if the extrinsic incubation period is shorter than the average mosquito lifespan, the control measures should be targeted towards reducing the mosquito biting rate. On the other hand, if the extrinsic incubation period is longer than the average mosquito lifespan, control measures targeting the mosquito death rate will be more effective. Intuitively, one might think that resources for malaria control should be allocated to the region with higher malaria transmission. However, our sensitivity analyses indicated that this is not always the case. In fact, if migration into the lower transmission patch is much faster than migration into the higher transmission patch, the lower transmission patch is potentially the better target for malaria control efforts. While human movement between regions poses challenges to malaria control and elimination, if estimates of relevant parameters in the model are known, including migration rates, our results can help inform which region to target and what type of control measure to implement for the greatest success.

Published by Elsevier Ltd.

1. Introduction

Malaria continues to pose a substantial public health problem worldwide, particularly in less developed countries. Malaria control, even in countries with relatively low malaria endemicity, proves to be a significant challenge (http://www.CDC.gov/Malaria/about/facts.html; Sachs and Malaney, 2002). Recently, the international community has increased its focus on reducing malaria burden worldwide, and malaria elimination has re-entered the lexicon of the malaria control community (Das and Horton, 2010; http://www.malariaeliminationgroup.org/about; Guinovart et al., 2006; New York Times, 2010; World and Media, 2011). In many countries, however, resources available towards implementing intervention strategies are extremely limited (Greenwood and Mutabingwa, 2002). Intervention strategies must be chosen to maximize the use of these limited funds to most efficiently reduce malaria burden. For many diseases, including malaria, human population movement contributes greatly to the spread and persistence of disease (Greenwood and Mutabingwa, 2002), and is therefore an important consideration when implementing

* Corresponding author. Tel.: +1 352 392 0281x307.
E-mail address: oprosper@ufl.edu (O. Prosper).

0022-5193/$ - see front matter Published by Elsevier Ltd.
doi:10.1016/j.jtbi.2012.02.010

intervention strategies (Woolhouse et al., 1997). Despite this, little is known about human movement patterns and their epidemiological consequences (Stoddard et al., 2009). In fact, the failure of the Global Malaria Eradication Programme in the 1950s and 1960s may be due, in part, to the failure to take into account human movement (Greenwood and Mutabingwa, 2002).

Human movement often links areas with different degrees of malaria transmission capacity (Martens and Hall, 2003). Local transmission dynamics often differs between areas (Stoddard et al., 2009) due to characteristics such as topography, mosquito species densities, pesticide use, availability of mosquito habitats, or differences in currently implemented intervention strategies (Githeko et al., 2006; Kulkarni et al., 2010); for example, urban areas typically have much lower malaria transmission than rural areas (Hay et al., 2005; Machault et al., 2010; Robert et al., 2003). Because human movement commonly links urban and rural systems that often exhibit dramatically different degrees of malaria transmission (Robert et al., 2003), urbanization may be an important driver in malaria dynamics.

Local transmission dynamics may influence the efficacy of intervention strategies. Because these transmission characteristics may vary between areas connected by human movement, human movement becomes important not only in terms of expected degree of importation, but also in terms of deciding where to target intervention strategies to most efficiently use resources.

In this study, we develop a mathematical model to address the implications of malaria movement between areas of potentially heterogeneous transmission characteristics, in order to determine effective targeted intervention strategies.

Mathematical models are a useful tool often applied to both identify control measures that are most important to implement, as well as quantify the effectiveness of different control strategies in controlling or eliminating malaria in endemic regions. For simplicity, most models consider transmission in one region of interest, with homogeneous transmission throughout the region. One of the first malaria models of this kind was the Ross–MacDonald model, which we describe in Section 2 (Bailey, 1982). In Section 2.1 we describe a modification of the Ross–Macdonald model, which is to be used in the human movement two patch model. While single-patch malaria models have proven to be very useful in the study of malaria dynamics, we know from many other systems that spatial structure can greatly influence the dynamics of interacting species (Hess, 1996; Holt, 1985; Pickett and Cadenasso, 1995), including pathogens and hosts (Ostfeld et al., 2005). Thus, there is a need to explore how malaria dynamics are affected by spatial heterogeneity and to use this information to inform intervention strategies. To address this need, in Section 2.2 we introduce a two-patch malaria metapopulation model based on the modified Ross–Macdonald model that allows for different local transmission characteristics and variable human migration rates between patches.

Metapopulation models have been used extensively in other systems to address common ecological issues, such as the effect of connectivity between areas (Hess, 1996) and the effect of migration on predator–prey dynamics (Adler, 1993). Similar models have also been used to investigate the implications these results might have for disease dynamics. Consequently, metapopulation models have been developed to explore the effect of migration on disease persistence. Hethcote (1976) found that migration could cause a disease to persist where it would otherwise die out if it were isolated using a two-patch SIS (Susceptible–Infected–Susceptible) model. We show in Section 2.3 that this result is also possible in our two-patch malaria model for a range of different immigration and emigration rates.

Metapopulation models of vector-borne disease have been previously studied to some extent as well. Cosner et al. (2009) considered two types of movement, termed Lagrangian and Eulerian, in their vector-borne disease metapopulation model. In the Lagrangian approach, individuals are considered residents of a particular patch and spend some fraction of the time visiting other patches. In the Eulerian approach, individuals are not tracked; while migration occurs between patches, this approach does not assign a "residence" to individuals in the population. Our two-patch model incorporates the Eulerian approach to modeling movement. Since it is uncommon for mosquitoes to move more than a kilometer throughout their lives (Costantini et al., 1996; Harrington et al., 2005; Midega et al., 2007; Muir and Kay, 1998; Russell et al., 2005) while humans often move many kilometers between villages and countries (Stoddard et al., 2009), we modeled human movement exclusively. In their malaria metapopulation model, Cosner et al. (2009) studied a special case of a two-patch malaria model with no transmission in one of the patches. In our study, we are interested in understanding how human movement affects malaria dynamics when two patches with different, nonzero transmission characteristics are connected by human migration. In Section 4.1, we parameterize our model using estimates from regions with varying levels of malaria endemicity, to encompass a variety of patch and human movement characteristics in the field.

In Section 2.3, we present an analytic expression derived from the two-patch model for the basic reproductive number, a threshold quantity determining whether a disease will persist or go extinct in a population. To assess the relative efficacy of different control measures and to determine where to target these control measures, we perform a sensitivity analysis of the basic reproductive number to different parameters in the model in Section 3. In Section 5, we perform a sensitivity analysis of the endemic equilibrium and compare these results to those of the analysis of the reproduction number. Chitnis et al. (2008) perform a similar sensitivity analysis using their single-patch malaria model. They found that under both high and low transmission settings, the basic reproductive number was most sensitive to the mosquito biting rate, and the equilibrium proportion of humans was most sensitive to the human recovery rate (Chitnis et al., 2008). However, our sensitivity analysis yielded a different result, likely due to different assumptions in the model formulation: the parameter the basic reproductive number is most sensitive to depends on the relative duration of the extrinsic incubation period and mosquito lifespan, and the human recovery rate was not the most important factor in the analysis of the endemic equilibrium. We also show that our intuition about where control measures should be implemented for the greatest success may not always be correct and that having an idea of the relative sizes of the migration rates between the two patches can provide insight into which patch should be the target of malaria control.

2. Ross–Macdonald model

In the Ross–Macdonald model, the rates at which the proportion of humans infected (x) and the proportion of mosquitoes infected (z) change over time are given by the following system of equations:

$$\frac{dz}{dt} = acx(1-z)-gz,$$

$$\frac{dx}{dt} = mabz(1-x)-rx, \tag{1}$$

where $1-z$ and $1-x$ are the proportion of mosquitoes and the proportion of humans that are susceptible, respectively (Bailey, 1982). We can rewrite these equations in terms of the number of

humans infected, rather than the proportion infected:

$$\frac{dz}{dt} = ac\frac{I}{N}(1-z)-gz,$$

$$\frac{dI}{dt} = mabz(N-I)-rI, \tag{2}$$

where N is the total size of the human population, and I is the number of humans in that population who are infected with malaria.

The parameter a is the human-biting rate (the rate at which mosquitoes bite humans). c is the human-to-mosquito transmission efficiency, that is, the probability, given a susceptible mosquito has bitten an infectious human that the mosquito becomes infected. Similarly, b is the mosquito-to-human transmission efficiency – the probability, given an infectious mosquito has bitten a susceptible human that the human becomes infected. The mosquito death rate is denoted by g. Finally, m denotes the ratio of the number of mosquitoes to humans, and r denotes the human recovery rate without treatment. Once a human recovers from malaria infection, they do not gain immunity, but instead are susceptible to re-infection.

Susceptible humans become infected at a rate $mabz$, and susceptible mosquitoes become infected at a rate acx. Infected humans are lost through recovery, and infected mosquitoes are lost through death. Because humans live much longer than the duration of a malaria infection and the lifespan of a mosquito, the human death rate is much smaller than any of the other parameters in this model, and hence is negligible. Similarly, we ignore human births.

2.1. Modifications to Ross–Macdonald model

Infected mosquitoes that do not survive the extrinsic incubation period of malaria never have the chance to transmit the disease. Depending on mosquito daily survival probabilities and duration of the extrinsic incubation period (which is dependent upon factors such as temperature), as many as half of infected mosquitoes may not survive to become infectious and able to transmit malaria (Githeko et al., 2006; Graves et al., 1990). To account for mosquito survival, the Ross–Macdonald model has been modified by replacing $(1-z)$ in the original model with $e^{-gn}-z$ (see Appendix 1 in Smith and McKenzie, 2004). In other words, the pool of mosquitoes is reduced from one to the proportion of individuals expected to survive the extrinsic incubation period, which has length n, if their death rate is g. As a final modification, we eliminate the mosquito equation by assuming that the infected mosquito population equilibrates much faster than the infected human population. This assumption is commonly used in malaria models because the mosquito dynamics (such as incubation period and death rate) operate on a much quicker timescale than human dynamics (such as the natural recovery rate) (Koella, 1991; Smith and McKenzie, 2004; Laxminarayan, 2004; Chiyaka et al., 2010). Thus, by assuming that the mosquito population dynamics is at equilibrium, the equations in (1) can be reduced to the single equation:

$$\frac{dI}{dt} = \frac{ma^2bcIe^{-gn}}{acI+gN}(N-I)-rI. \tag{3}$$

To simplify the notation, we let $\alpha \doteq mabe^{-gn}$ and $\beta \doteq ac$ so that Eq. (3) can be written as

$$\frac{dI}{dt} = \frac{\alpha\beta I}{\beta I+gN}(N-I)-rI. \tag{4}$$

2.2. Two-patch malaria model

Eq. (4) is used in our two-patch model to describe the disease dynamics within each patch. Each patch contains a human population of size N_i composed of S_i susceptible humans and I_i infected humans, with migration from patch j to patch i occurring at a rate k_{ij}, regardless of the health status of an individual.

In this model, transmission occurs only between individuals within a patch; individuals in a given patch cannot directly infect individuals in other patches. Movement from patch j to patch i occurs at a per capita rate k_{ij}, and individuals are identified simply as being in a given patch at a given time; individuals do not have a home patch. This approach to modeling movement is related to the Eulerian approach in fluid dynamics, and can be contrasted with movement models related to the Lagrangian approach in fluid dynamics, which has also been used to model human movement in disease metapopulation models (Cosner et al., 2009). While the Eulerian approach does not track individuals and individuals cannot infect across patches without changing their resident patch, the Lagrangian approach assigns an unchanging resident patch to individuals (Cosner et al., 2009). Individuals then spend a proportion of time in other patches, transmitting disease to individuals in other patches.

The choice between Lagrangian and Eulerian movement models depends upon spatial scale and types of population movement modeled. Movement on smaller spatial scales tends to occur more frequently, between multiple patches in rapid succession (such as the daily commute to work or school, or seasonal movements) (Stoddard et al., 2009). These movements are termed circulation in classical population movement typology (Prothero, 1977) and involve no change of residence (Martens and Hall, 2003). In these cases, the Lagrangian approach is generally more appropriate. Rarer, more permanent movement (termed migration Martens and Hall, 2003; Prothero, 1977), which is more appropriately modeled using the Eulerian approach, tends to occur on much larger spatial scales (for example, due to individuals changing residence due to urbanization or displacement, Stoddard et al., 2009).

Although most human movement consists of short-term visits, our objective was to study the effect of longterm migration on decisions concerning malaria control. Migration due to processes that occur on large spatial scales, such as urbanization and transborder migration, is an important component of malaria systems. The degree of transborder movement between two countries requires that any elimination campaign be highly coordinated (Keating et al., 2010). By using an Eulerian approach to movement, we may examine the effect of transborder migration on malaria dynamics, which has implications for international malaria control efforts (Tatem and Smith, 2010).

Combining the conceptualization of the model in Fig. 1 and the Eulerian framework for movement with the disease-dynamics given by the modified Ross–Macdonald model, we arrive at the following system of differential equations to describe the malaria dynamics of a human population distributed between two patches:

$$\frac{dS_1}{dt} = -\frac{\alpha_1\beta_1 I_1}{\beta_1 I_1+g_1N_1}S_1+r_1I_1-k_{21}S_1+k_{12}S_2,$$

$$\frac{dS_2}{dt} = -\frac{\alpha_2\beta_1 I_2}{\beta_2 I_2+g_2N_2}S_2+r_2I_2-k_{12}S_2+k_{21}S_1,$$

$$\frac{dI_1}{dt} = \frac{\alpha_1\beta_1 I_1}{\beta_1 I_1+g_1N_1}S_1-r_1I_1-k_{21}I_1+k_{12}I_2,$$

$$\frac{dI_2}{dt} = \frac{\alpha_2\beta_1 I_2}{\beta_2 I_2+g_2N_2}S_2-r_2I_2-k_{12}I_2+k_{21}I_1.$$

In the system above, the population size of patch i is $N_i = S_i+I_i$, and the total population size is $N = N_1+N_2$. Note that $dN/dt = 0$, hence N is constant. A description of the model parameters can be found in Table 1.

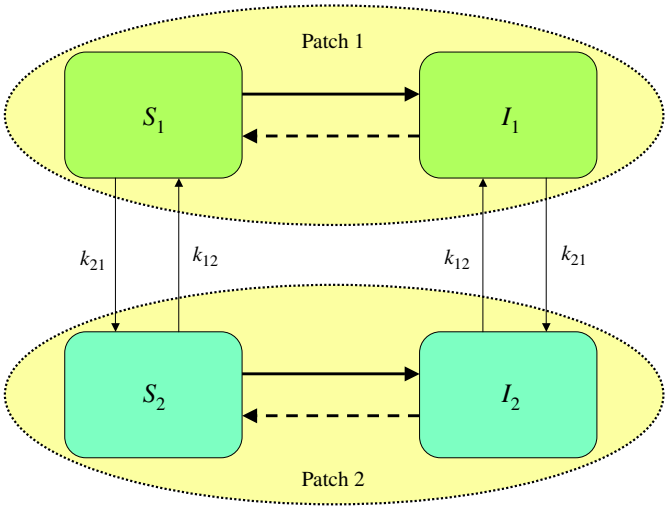

Fig. 1. Disease dynamics in a human population. Solid bold arrows indicate the acquisition of a new infection; dashed arrows indicate recovery; solid thin arrows indicate migration between patches.

Table 1
Description of model parameters in patch i.

Parameters	Description
m_i	Ratio of the number of mosquitoes to the number of humans
a_i	Human biting rate
$m_i a_i$	Number of mosquito bites on a human per unit of time
b_i	Transmission efficiency from mosquito to human
c_i	Transmission efficiency from human to mosquito
g_i	Natural death rate of mosquitoes
n_i	Length of mosquito incubation period
α_i	$m_i a_i b_i e^{-g_i n}$
β_i	$a_i c_i$
r_i	Natural human recovery rate
k_{ij}	Migration rate from patch j to patch i

Since $N_1' = -k_{21}N_1 + k_{12}N_2$ implies that $N_2^* = (k_{21}/k_{12})N_1^*$, where N_1^* and N_2^* denote the equilibrium values of N_1 and N_2, respectively, and $N_1^* + N_2^* = N$, we have that $N_1^* = (k_{12}/(k_{12}+k_{21}))N$ and $N_2^* = (k_{21}/(k_{12}+k_{21}))N$ at equilibrium. Thus, since $S_1 = N_1$ and $S_2 = N_2$ when there is no disease, the disease-free equilibrium (DFE) of the above system is $(S_1^*, I_1^*, S_2^*, I_2^*)_{DFE} = ((k_{12}/(k_{12}+k_{21}))N, 0, (k_{21}/(k_{12}+k_{21}))N, 0)$.

If $dI_1/dt = 0$ and malaria is absent in patch 1 ($I_1 = 0$), then $I_2^* = 0$ when $k_{12} > 0$. Likewise, if $dI_2/dt = 0$ and malaria is absent in patch 2 ($I_2 = 0$), then I_1^* must be zero when $k_{21} > 0$. Thus, at equilibrium, malaria cannot be present in one patch and absent in the other, provided that the migration rates are nonzero.

2.3. The basic reproductive number R_0

The basic reproductive number, R_0, is traditionally defined to be the number of secondary cases resulting from one infectious individual in an otherwise fully susceptible population. In a model without acquired immunity, R_0 provides a threshold criteria for persistence of the disease in a population. If $R_0 < 1$, the disease will become extinct. If $R_0 > 1$, the disease will persist in the population. The basic reproductive number for the modified Ross–Macdonald model (3) is $\alpha\beta/gr$ where $\alpha = mabe^{-gn}$ and $\beta = ac$. Thus without migration, patch i in the two-patch model will have its own isolated-patch reproduction number $R_{0i} = \alpha_i\beta_i/g_i r_i$, where $\alpha_i = m_i a_i b_i e^{-g_i n_i}$ and $\beta_i = a_i c_i$ for $i = 1,2$. Using the next-generation approach (Diekmann et al., 1990; van den Driessche and Watmough, 2002), we find that the basic reproductive number (the dominant eigenvalue of the next generation matrix) for our two-patch model with migration is given by the expression:

$$R_0 = \frac{1}{2\sigma}\left[s_1t_2 + s_2t_1 + \sqrt{(s_1t_2 + s_2t_1)^2 - 4s_1s_2\sigma}\right], \tag{5}$$

$$R_0 = \frac{1}{2\sigma}\left[s_1t_2 + s_2t_1 + \sqrt{(s_1t_2 - s_2t_1)^2 + 4s_1s_2k_{12}k_{21}}\right], \tag{6}$$

where

$$\sigma = k_{12}r_1 + k_{21}r_2 + r_1r_2,$$

$$s_i = \frac{\alpha_i\beta_i}{g_i} = r_i * R_{0i},$$

$$t_i = r_i + k_{ji}$$

for $i = 1,2$. Although this expression for R_0 does not possess the biological interpretation of the traditional definition, it still provides the same useful persistence–extinction threshold criterion.

Observe that when there is no migration between patches, $k_{12} = k_{21} = 0$, then $R_0 = \max\{\alpha_1\beta_1/r_1g_1, \alpha_2\beta_2/r_2g_2\} = \max\{R_{01}, R_{02}\}$, the larger of the two isolated-patch reproductive numbers. Moreover, the value of the global reproductive number R_0 for this two-patch model is always between the two isolated-patch reproductive numbers R_{01} and R_{02} when migration between the two patches is present. In one parameterization of their two-patch malaria model with Lagrangian movement, Cosner et al. (2009) found that it was possible to have a scenario in which each isolated patch reproduction number (R_{01} and R_{02}) is less than 1, yet the global reproduction number R_0 is larger than one. This finding illustrates that some models predict that it may be possible to have a system where without migration, the disease goes extinct in both patches, but once a certain level of migration is introduced, the disease becomes endemic. However, as is stated in the following Theorem, our two-patch model, which assumes Eulerian rather than Lagrangian movement, predicts that R_0 will always be bounded by the isolated patch reproduction numbers. A similar result has been derived for direct transmission epidemic models with Lagrangian-type movement (Arino and van den Driessche, 1993, 2003; Salmani and van den Driessche, 2006).

Theorem 2.3.1. *If $R_{01} > R_{02}$, then for all pairs of migration rates $(k_{12}, k_{21}) \in [0,\infty) \times [0,\infty)$,*

$$\max\left\{\frac{R_{01}}{1 + \frac{k_{21}}{r_1}}, R_{02}\right\} \le R_0 \le R_{01}.$$

Proof. $R_{01} > R_{02}$ implies that $s_1/r_1 > s_2/r_2$. Thus, by assumption we have that $s_1r_2 > s_2r_1$. We first evaluate R_0 at certain points on the boundary of the domain $[0,\infty) \times [0,\infty)$. From Eq. (6), we have

$$R_0(k_{12}, 0) = \frac{1}{2r_1t_2}(s_1t_2 + s_2r_1 + |s_1t_2 - s_2r_1|). \tag{7}$$

Since by assumption $s_1r_2 > s_2r_1$, and because $t_2 = r_2 + k_{12} \ge r_2$, we know that $s_1t_2 - s_2r_1 > 0$, and so $|s_1t_2 - s_2r_1| = s_1t_2 - s_2r_1$. Thus, Eq. (7) simplifies to $R_0(k_{12}, 0) = R_{01}$ for all $k_{12} \in [0,\infty)$.

Similarly,

$$R_0(0, k_{21}) = \frac{1}{2r_2t_1}(s_1r_2 + s_2t_1 + |s_1r_2 - s_2t_1|) = \frac{1}{r_2t_1} \cdot \max\{s_1r_2, s_2t_1\}$$

$$= \max\left\{\frac{s_1}{t_1}, \frac{s_2}{r_2}\right\} = \max\left\{\frac{R_{01}}{1 + \frac{k_{21}}{r_1}}, R_{02}\right\}. \tag{8}$$

Thus, $R_{02} \le R_0(0, k_{21}) \le R_{01}$, for all k_{21} in the interval $[0,\infty)$.

Consider the function

$$f(x)=\sigma x^2-(s_1t_2+s_2t_1)x+s_1s_2. \tag{9}$$

f is precisely the characteristic polynomial of the next-generation matrix used to derive R_0 in Eq. (5). R_0 is the larger of the two roots of the concave-up parabola $f(x)$. Consequently, $f(R_0)=0$ and $f'(R_0)>0$. From this we know that for any real number x^* satisfying the inequality $f(x^*)<0$, then x^* must be less than R_0. On the other hand, if x^* is such that $f(x^*)>0$ and $f'(x^*)>0$, then x^* is greater than R_0.

Suppose k_{12} and k_{21} are positive. Then,

$$\begin{aligned}f(R_{01})&=f\left(\frac{s_1}{r_1}\right)=\sigma\left(\frac{s_1}{r_1}\right)^2-(s_1t_2+s_2t_1)\frac{s_1}{r_1}+s_1s_2\\&=\frac{s_1}{r_1}\left[(k_{12}r_1+k_{21}r_2+r_1r_2)\frac{s_1}{r_1}-(s_1t_2+s_2t_1)+s_2r_1\right]\\&=\frac{s_1}{r_1}\left[s_1k_{12}+s_1\frac{k_{21}r_2}{r_1}+s_1r_2-(s_1t_2+s_2t_1)+s_2r_1\right]\\&=\frac{s_1}{r_1}\left[s_1t_2+s_1\frac{k_{21}r_2}{r_1}-(s_1t_2+s_2t_1)+s_2r_1\right]\\&=\frac{s_1}{r_1}\left(\frac{s_1r_2}{r_1}k_{21}-s_2k_{21}\right)\\&=\frac{s_1k_{21}}{r_1^2}(s_1r_2-s_2r_1).\end{aligned}$$

By assumption, $s_1r_2-s_2r_1>0$, hence $f(R_{01})>0$. Similarly, we can show that

$$f(R_{02})=f\left(\frac{s_2}{r_2}\right)=\frac{s_2k_{12}}{r_2^2}(s_2r_1-s_1r_2), \tag{10}$$

$$f\left(\frac{R_{01}}{1+\frac{k_{21}}{r_1}}\right)=-\left(\frac{s_1}{t_1}\right)^2k_{12}k_{21}. \tag{11}$$

Clearly

$$f\left(\frac{R_{01}}{1+\frac{k_{21}}{r_1}}\right)<0$$

and since $s_1r_2-s_2r_1>0$, we also have that $f(R_{02})<0$.

Now, $f'(x)=2\sigma x-(s_1t_2+s_2t_1)$. So,

$$f'(R_{01})=f'\left(\frac{s_1}{r_1}\right)=2\sigma\frac{s_1}{r_1}-(s_1t_2+s_2t_1), \tag{12}$$

$$f'(R_{01})=2(r_1r_2+r_1k_{12}+r_2k_{21})\frac{s_1}{r_1}-s_1r_2-s_1k_{12}-s_2r_1-s_2k_{21}, \tag{13}$$

$$f'(R_{01})=(s_1r_2-s_2r_1)+s_1k_{12}+(2s_1r_2-s_2r_1)\frac{k_{21}}{r_1}. \tag{14}$$

Again, since $s_1r_2-s_2r_1>0$, $f'(R_{01})>0$.

Thus, for k_{12} and k_{21} positive, $f(R_{02})<0$ and

$$f\left(\frac{R_{01}}{1+\frac{k_{21}}{r_1}}\right)<0$$

implies that

$$R_0>\max\left(R_{02},\frac{R_{01}}{1+\frac{k_{21}}{r_1}}\right).$$

Also, $f(R_{01})>0$ and $f'(R_{01})>0$ implies that $R_0<R_{01}$. We have already shown that $R_0(k_{12},0)=R_{01}$ and $R_0(0,k_{21})=\max\{R_{01}/(1+(k_{21}/r_1)),R_{02}\}$. Therefore, for all non-negative k_{12} and k_{21}, $\max\{R_{01}/(1+(k_{21}/r_1)),R_{02}\}\le R_0\le R_{01}$. □

Theorem 2.3.2. *Suppose $R_{01}>R_{02}$. Consider $R_0(k_{12},k_{21})$ to be a function of both migration rates k_{12} and k_{21}, where $k_{12},k_{21}\in[0,\infty)$. For a fixed κ in the interval $[0,\infty)$, $R_0(k_{12},\kappa)$ is an increasing function of k_{12} and $R_0(\kappa,k_{21})$ is a decreasing function of k_{21}.*

Proof. We have shown in the proof of Theorem 2.3.1 that $R_0(0,\kappa)=\max\{R_{01}/(1+(\kappa/r_1)),R_{02}\}$ and $R_0(k_{12},\kappa)>\max\{R_{01}/(1+(\kappa/r_1)),R_{02}\}$ for $k_{12}>0$. Thus $R_0(k_{12},\kappa)\ge R_0(0,\kappa)$ for all $k_{12}\ge0$. So, we need only to show that $R_0(k_{12},\kappa)$ is monotonic in k_{12} to show that it is an increasing function in k_{12}. Similarly, from Theorem 2.3.1 we also know that $R_0(\kappa,0)=R_{01}\ge R_0(\kappa,k_{21})$ for all non-negative k_{21}. So again, we need only show that $R_0(\kappa,k_{21})$ is monotonic in k_{21} to show that it is a decreasing function in k_{21}.

First, we show that $R_0(k_{12},\kappa)$ is monotonic in k_{12}.

Since $R_0(k_{12},\kappa)$ is continuous in k_{12}, it is monotonic with respect to k_{12} if for every $C\in(0,\infty)$ such that $R_0(k_{12},\kappa)=C$ has a non-negative solution $k_{12}\in[0,\infty)$, then this solution is unique.

Suppose $R_0(k_{12},\kappa)=C$. Then, by the definition of R_0 (Eq. (5)), we have that

$$\frac{1}{2\sigma}\left(q+\sqrt{q^2-4s_1s_2\sigma}\right)=C, \tag{15}$$

where $q=s_1t_2+s_2t_1=s_1(r_2+k_{12})+s_2(r_1+\kappa)$ and $\sigma=r_1r_2+r_1k_{12}+r_2\kappa$.

Eq. (15) implies that

$$\sigma C^2-qC+s_1s_2=0. \tag{16}$$

Observe that both σ and q are linear in k_{12}. Thus, Eq. (16) is linear in k_{12}, implying that if there exists a $k_{12}\in[0,\infty)$ that is a solution to Eq. (16), then this solution is unique. Hence, $R_0(k_{12},\kappa)$ is monotonic for each $\kappa\in[0,\infty)$. By the same argument, $R_0(\kappa,k_{21})$ is monotonic for each $\kappa\in[0,\infty)$.

Since $R_0(k_{12},\kappa)$ is monotonic for non-negative k_{12} and $R_0(0,\kappa)\le R_0(k_{12},\kappa)$, for each fixed $k_{21}=\kappa\in[0,\infty)$, R_0 is an increasing function of k_{12}. Likewise, since $R_0(\kappa,0)\ge R_0(\kappa,k_{21})$ for non-negative k_{21}, for each fixed $k_{12}=\kappa\in[0,\infty)$, R_0 is a decreasing function of k_{21}. □

The proof of Theorem 2.3.1, assuming that $R_{01}>R_{02}$, also shows that the minimum value of $R_0(k_{12},k_{21})$ on the domain $[0,\infty)\times[0,\kappa)$ is $\max\{R_{01}/(1+(\kappa/r_1)),R_{02}\}$ and the maximum value is R_{01}. Thus, if $R_{02}<1$ and $R_{01}/(1+(\kappa/r_1))>1$ for some $\kappa>0$ (and hence $R_{01}>1$), then $R_0(k_{12},k_{21})>1$ for all migration pairs (k_{12},k_{21}) in $[0,\infty)\times[0,\kappa)$. This indicates that it is possible to have a situation in which without migration, the disease dies out in one patch but not the other, yet with migration the disease persists in both patches for all $k_{12}\ge0$ and for $0\le k_{21}\le\kappa$.

If R_{02} and $R_{01}/(1+(\kappa/r_1))$ are less than one but $R_{01}>1$, then for some migration rate pairs (k_{12},k_{21}), R_0 will be larger than one, and for other pairs, R_0 will be less than one. Furthermore, there exists a value $\kappa^*<\kappa$ such that $R_0>1$ for all (k_{12},k_{21}) in $[0,\infty)\times[0,\kappa^*)$.

Finally, if R_{02} and R_{01} are both less than one, then R_0 will always be less than one, regardless of the migration rates between patches.

3. Sensitivity analysis

An elasticity analysis of the basic reproduction number and endemic equilibrium provides a means of determining which parameters are the best targets for malaria control for elimination strategies and reduction of prevalence, respectively. The parameters

that serve as the best targets can then be used to inform which control strategies should be used, through selection of malaria interventions that target those parameters.

Population biologists make use of sensitivity and elasticity analyses to evaluate the effect of perturbations in a population fecundity, growth, and survival on the overall growth of the population, and to determine which life stage a population's growth is most sensitive to Heppel et al. (2000) and van Tienderen (2000). The sensitivity of a quantity λ to a parameter p is calculated as $s=\partial\lambda/\partial p$, and is used to determine the amount of change that occurs in λ in response to changes in elements p; sensitivity can then be used to compare how absolute changes in various parameters affect λ (deKroon et al., 1986). However, we cannot easily compare sensitivities with respect to parameters of different scales. For example, the effect of a 0.5 increase in transmission efficiency (measured from 0 to 1) in this model is not easily comparable to the effect of a 0.5 increase in mosquito incubation period; a 0.5 increase in transmission represents a much larger change to the system. Therefore, an alternate measure that allows for comparison of parameters with different scales is preferable; in this study, elasticity is used. Elasticity is the proportional change in λ resulting from a proportional change in a. Because elasticity is determined using the proportion rather than absolute change in a parameter p, the effect of parameters on λ, or in this case, R_0, can be compared, even if the parameters are very different in scale. Thus, we compute the elasticity of R_0 to a parameter p, rather than the sensitivity, to compare parameters of different orders of magnitude and different units:

$$\varepsilon_p=\frac{\partial R_0}{\partial p}\frac{p}{R_0}. \tag{17}$$

The value ε_p describes how much, and in what way (positively or negatively), the reproduction number will be affected by a small change in a parameter value p. More precisely, we can interpret the elasticity as follows: if the elasticity of a quantity λ with respect to a parameter p is ε_p, then a 1% change in p will result in an ε_p% change in λ. We compute the analytic expressions of the elasticities for each parameter in both the single patch model without migration and the two-patch model so that we may draw some general conclusions about the relative importance of each parameter in these two scenarios.

3.1. Elasticities for a single patch without migration

From Eq. (17) and the single-patch expression for R_0, ma^2bce^{-gn}/rg, we find that

$$\varepsilon_m=\varepsilon_b=\varepsilon_c=1,$$

$$\varepsilon_r=-1,$$

$$\varepsilon_a=2,$$

$$\varepsilon_g=-(gn+1),$$

$$\varepsilon_n=-gn.$$

Thus, we have (for $p=m,b,c$) that $|\varepsilon_n|<1=|\varepsilon_r|=\varepsilon_p<|\varepsilon_g|<\varepsilon_a$ if $n<1/g$, where n is the incubation period and $1/g$ is the expected mosquito lifespan. If $1/g<n<2/g$, in other words if the incubation period is longer than the expected mosquito lifespan but shorter than twice this lifespan, then $1=|\varepsilon_r|=\varepsilon_p<|\varepsilon_n|<\varepsilon_a<|\varepsilon_g|$. Finally, if $n>2/g$, then $1=|\varepsilon_r|=\varepsilon_p<\varepsilon_a<|\varepsilon_n|<|\varepsilon_g|$.

Generally, theoretical studies have found that the basic reproduction number in malaria models is most elastic to the human biting rate, which plays a major role as it influences both transmission to mosquitoes and transmission to humans; this is reflected in the fact that the elasticity of R_0 to a is double that of m, b, or c (Chitnis et al., 2008). Using the interpretation of elasticity in terms of percentages, since $\varepsilon_a=2$, a 1% increase in a will result in a 2% increase in R_0. On the other hand, $\varepsilon_m=1$ implies that the same 1% increase in m will result in only a 1% increase in R_0. In our model, however, R_0 is most sensitive to g when $n>1/g$; i.e. when the incubation period is longer than the average mosquito lifespan. Unlike the elasticities related to the parameters m,a,b,c, and r, the elasticities of R_0 with respect to the mosquito death rate g and incubation period n are linear functions of both g and n. Thus, increasing mosquito death rate or lengthening the extrinsic incubation period enhances the effect of such control measures on R_0.

3.2. Elasticities for the two-patch metapopulation model

The analytic expressions for the elasticities in the two-patch model with migration, while more complicated in form than those of the single-patch model, provide some insight into the relative importance of the model parameters.

For $p_i=m_i,a_i,b_i,c_i,g_i,n_i$, we have that

$$\frac{\partial R_0}{\partial p_1}=\frac{\partial s_1}{\partial p_1}\cdot\frac{1}{2\sigma}\left[t_2\left(1+\frac{s_1t_2-s_2t_1}{\sqrt{\tau}}\right)+\frac{2s_2k_{12}k_{21}}{\sqrt{\tau}}\right], \tag{18}$$

$$\frac{\partial R_0}{\partial p_2}=\frac{\partial s_2}{\partial p_2}\cdot\frac{1}{2\sigma}\left[t_1\left(1-\frac{s_1t_2-s_2t_1}{\sqrt{\tau}}\right)+\frac{2s_1k_{12}k_{21}}{\sqrt{\tau}}\right], \tag{19}$$

where $\tau=(s_1t_2-s_2t_1)^2+4s_1s_2k_{12}k_{21}$, $\partial s_i/\partial p_i=s_i/p_i$ for $p_i=m_i,b_i,c_i$, $\partial s_i/\partial a_i=2s_i/a_i$, $\partial s_i/\partial g_i=-s_i((g_in_i+1)/g_i)$, and $\partial s_i/\partial n_i=-g_is_i$.

Thus, the elasticities for $p_i=m_i,b_i,c_i$ are given by the expressions:

$$\varepsilon_{p_1}=\frac{s_1}{2\sigma R_0}\cdot\left[t_2\left(1+\frac{s_1t_2-s_2t_1}{\sqrt{\tau}}\right)+\frac{2s_2k_{12}k_{21}}{\sqrt{\tau}}\right], \tag{20}$$

$$\varepsilon_{p_2}=\frac{s_2}{2\sigma R_0}\cdot\left[t_1\left(1-\frac{s_1t_2-s_2t_1}{\sqrt{\tau}}\right)+\frac{2s_1k_{12}k_{21}}{\sqrt{\tau}}\right], \tag{21}$$

and

$$\varepsilon_{a_i}=2\varepsilon_{p_i}, \tag{22}$$

$$\varepsilon_{g_i}=-\varepsilon_{p_i}(g_in_i+1), \tag{23}$$

$$\varepsilon_{n_i}=-g_in_i\varepsilon_{p_i}. \tag{24}$$

For $k_{12},k_{21}\neq 0$, because $\sqrt{\tau}\geq|s_1t_2-s_2t_1|$, $(1+((s_1t_2-s_2t_1)/\sqrt{\tau}))$ and $(1-((s_1t_2-s_2t_1)/\sqrt{\tau}))$, which appear in the expressions for ε_{p_1} and ε_{p_2}, respectively, lie in the interval $(0,2)$. Thus, ε_{p_i} is positive for $p_i=m_i,a_i,b_i,c_i$ and negative for $p_i=g_i,n_i$. Since $g_in_i+1>1$, $\varepsilon_{p_i}<\varepsilon_{a_i}<|\varepsilon_{g_i}|$ if $n_i>1/g_i$, and $\varepsilon_{p_i}<|\varepsilon_{g_i}|<\varepsilon_{a_i}$ if $n_i<1/g_i$.

The elasticity for the remaining model parameters r_i,k_{ij}, and n are given by

$$\varepsilon_{r_1}=\frac{r_1}{2\sigma R_0}\left[s_2\left(1-\frac{s_1t_2-s_2t_1}{\sqrt{\tau}}\right)\right]-\frac{r_1t_2}{\sigma},$$

$$\varepsilon_{r_2}=\frac{r_2}{2\sigma R_0}\left[s_1\left(1+\frac{s_1t_2-s_2t_1}{\sqrt{\tau}}\right)\right]-\frac{r_2t_1}{\sigma},$$

$$\varepsilon_{k_{21}}=\frac{k_{21}}{2\sigma R_0}\left[s_2\left(1-\frac{s_1t_2-s_2t_1}{\sqrt{\tau}}\right)+\frac{2s_1s_2k_{12}}{\tau}\right]-\frac{r_2k_{21}}{\sigma},$$

$$\varepsilon_{k_{12}}=\frac{k_{12}}{2\sigma R_0}\left[s_2\left(1+\frac{s_1t_2-s_2t_1}{\sqrt{\tau}}\right)+\frac{2s_1s_2k_{21}}{\tau}\right]-\frac{r_1k_{12}}{\sigma},$$

$$\varepsilon_{n_1}=-\frac{s_1g_1n_1}{2\sigma R_0}\left[t_2\left(1+\frac{s_1t_2-s_2t_1}{\sqrt{\tau}}\right)+2s_2k_{12}k_{21}\right],$$

$$\varepsilon_{n_2}=-\frac{s_2g_2n_2}{2\sigma R_0}\left[t_1\left(1-\frac{s_1t_2-s_2t_1}{\sqrt{\tau}}\right)+2s_1k_{12}k_{21}\right].$$

If $r_i<k_{ji}$, then $\varepsilon_{r_i}<\varepsilon_{k_{ji}}$.

Finally, we found that the elasticities of R_0 with respect to a pair of parameters (p_1,p_2) sum to the corresponding isolated-patch elasticity ε_p, for the parameters $p=m,a,b,c$. This result is given in the following theorem.

Theorem 3.2.1. *For* $p_i=m_i,b_i,c_i$, $\varepsilon_{p_1}+\varepsilon_{p_2}=1$.

Proof.

$$2\sigma R_0(\varepsilon_{p_1}+\varepsilon_{p_2})=s_1t_2+s_2t_1+\frac{(s_1t_2-s_2t_1)^2+4s_1s_2k_{12}k_{21}}{\sqrt{\tau}}, \tag{25}$$

$$2\sigma R_0(\varepsilon_{p_1}+\varepsilon_{p_2})=s_1t_2+s_2t_1+\frac{\tau}{\sqrt{\tau}}, \tag{26}$$

$$2\sigma R_0(\varepsilon_{p_1}+\varepsilon_{p_2})=s_1t_2+s_2t_1+\sqrt{\tau}, \tag{27}$$

$$2\sigma R_0(\varepsilon_{p_1}+\varepsilon_{p_2})=2\sigma R_0. \tag{28}$$

Thus, dividing both sides of the above equation by $2\sigma R_0$ yields $\varepsilon_{p_1}+\varepsilon_{p_2}=1$. □

Since for $p_i=m_i,b_i,c_i$, $\varepsilon_{a_i}=2\varepsilon_{p_i}$, $\varepsilon_{g_i}=(g_in_i+1)\varepsilon_{p_i}$, and $\varepsilon_{n_i}=(g_in_i)\varepsilon_{p_i}$, Theorem 3.2.1 implies that $\varepsilon_{a_1}+\varepsilon_{a_2}=2$, $\min\{g_1n_1,g_2n_2\}+1\le\varepsilon_{g_1}+\varepsilon_{g_2}\le\max\{g_1n_1,g_2n_2\}+1$, and $\min\{g_1n_1,g_2n_2\}\le\varepsilon_{n_1}+\varepsilon_{n_2}\le\max\{g_1n_1,g_2n_2\}$.

While the relationship between the elasticities for parameters m_i,a_i,b_i,c_i and g_i in patch i are clear, the relationship between the remaining parameters (r_i and k_{ji}) and the relationship between parameters of different patches, are not obvious from the analytic expressions presented in this section. In the following sections we will estimate parameter values and use these estimates to derive elasticities for all model parameter values under various scenarios, which we will define using combinations of different parameter sets corresponding to high transmission, low transmission, fast migration, and slow migration.

4. Numerical results

4.1. Parameter estimates

Realistic parameter values were needed to gain an understanding of how spatial heterogeneity in malaria transmission affects the prevalence of malaria, malaria transmission, and malaria control in our two-patch model. We compiled baseline parameter values for four different situations, estimated from published studies. First, we compiled values for high transmission areas, and low transmission areas. High transmission parameters were gathered from studies in sub-Saharan Africa. Low transmission parameters were taken from studies in the Americas, especially South America, where the number of cases is generally low.

Among regions that are considered high transmission, there is still a lot of variability in their levels of malaria transmission. Thus, to encompass some of this variability, we compiled parameters associated with the dry season in a high transmission region and parameters associated with the wet season in a high transmission region. Similarly, not all low transmission regions can be described by the same set of transmission parameters. So, we again compiled dry season and wet season parameters for a low transmission region. Using these estimates from different seasons in both high and low transmission areas, we obtained four parameter sets representative of a high-transmission/wet-conditions patch, high-transmission/dry-conditions patch, low-transmission/wet-conditions patch, and low-transmission/dry-conditions patch (Table 2).

The ratio of mosquitoes to humans m was not directly calculated for the wet and dry conditions. Instead, the value ma was measured in various field studies by estimating the average number of bites on a human per night. The proportion of bites on humans out of all bites from the vector species was divided by the average time between blood meals to calculate a, the human biting rate. By knowing ma and a, we calculated m.

The difference in ma between wet and dry conditions was not directly found for the high transmission scenario; however, field studies have shown that the biting rate on humans in the wet season is tenfold that of the dry season (Smith et al., 1993); we assumed ma for the dry season was 1/10 that of the wet season, and determined m from the resultant ma value.

For each of our four baseline parameter sets, we calculated the basic reproductive number for an isolated patch with those parameter values (see Table 3).

These four parameter sets were used to describe the within-patch malaria transmission parameters in our two-patch model. Using the four parameter sets and the analytic expressions derived for R_{01} and R_{02}, we calculated and used these isolated-patch reproductive number estimates as a baseline to compare the global R_0 value to in different parameterizations of the two-patch model. We present results for three scenarios: in the first two scenarios patch one is high transmission and patch two is low transmission. In the first scenario, both patches have dry

Table 3
R_0 for the four scenarios.

Season	High transmission	Low transmission
Wet	187.15	7.03
Dry	3.80	0.70

Table 2
Wet and dry condition estimates of model parameters for low and high transmission settings. Note: m was not directly determined from field studies. $m*a$ for dry conditions is known from Fontenille et al. (1997). We assume for wet conditions the value to be 10 times greater according to Smith et al. (1993).

Parameters	Low			High		
	Wet	Dry	Reference	Wet	Dry	Reference
m_i	176.19	17.619		395.45	60.81	Molineaux and Gramiccia (1980)
a_i	0.105	0.105	Loyola et al. (1993)	0.41	0.265	Lindsay et al. (1991), Molineaux and Gramiccia (1980)
m_ia_i	18.5	1.85	Fontenille et al. (1997)	161.1477	16.114	Lindsay et al. (1991)
b_i	0.1	0.1	Beier et al. (1991)	0.097	0.097	Molineaux and Gramiccia (1980)
c_i	0.214	0.214		0.214	0.214	Collins et al. (1977), Bonnet et al. (2000)
g_i	0.167	0.167	Graves et al. (1990), Rodriguez et al. (1992)	0.181	0.26	Lindsay et al. (1991)
n_i	10 days	10 days		10 days	10 days	Molineaux and Gramiccia (1980)
r_i	1/150 days	1/150 days	Collins and Jeffery (2003), Bekessy et al. (1976)	1/150 days	1/150 days	

conditions. In the second scenario, both patches experience wet conditions. Finally, both patches are identical low transmission, dry condition patches in the third scenario.

4.2. Effect of migration on R_0

We first calculated the global R_0 according to Eq. (5), with each patch using parameters from one of the parameter sets in Table 2. We varied k_{12} and k_{21} to examine the patterns of global R_0 with varying migration rates. Assuming for simplicity that $R_{01} > R_{02}$, from Section 2.3, we know that $\min(R_0) = \max\{R_{01}/(1+(\kappa/r_1)), R_{02}\}$ for $(k_{12},k_{21}) \in [0,\infty) \times [0,\kappa)$, and $\max(R_0) = R_{01}$. Using this fact about the maximum and minimum values of R_0 along with our estimates of the isolated-patch reproductive numbers under the four patch characteristics identified in Table 3 (High-Wet, High-Dry, Low-Wet, Low-Dry), we can determine what the range of R_0 will be with migration under each scenario.

Numerical simulation of the global R_0 (Fig. 2) as a function of the migration rates suggests that if the migration terms k_{12}, k_{21} are zero, the global R_0 is equal to R_{01} (assuming $R_{01} > R_{02}$). For $k_{21} > 0$, as k_{12} increases, the global R_0 gets closer to the value of R_{01}. This is likely because as k_{12} increases, a higher proportion of individuals expose themselves to the transmission characteristics of patch 1, causing that patch to contribute more to the global R_0. Similarly, as k_{21} increases, the global R_0 becomes closer to the minimum R_0 value, R_{02}. These numerical findings are in agreement with the proof of Theorem 2.3.1. So, if patch 2 has $R_{02} < 1$, but $R_{01} > 1$ and $k_{12} \gg k_{21}$, more people will be exposed to the transmission characteristics of patch 1 than of patch 2, making it more likely that the disease will persist in both patches. The opposite is also true; if many more individuals are moving into patch 2 than patch 1 ($k_{21} \gg k_{12}$), the disease is likely to go extinct, since more people are exposed to the transmission characteristics of the low transmission patch than to those of the high transmission patch.

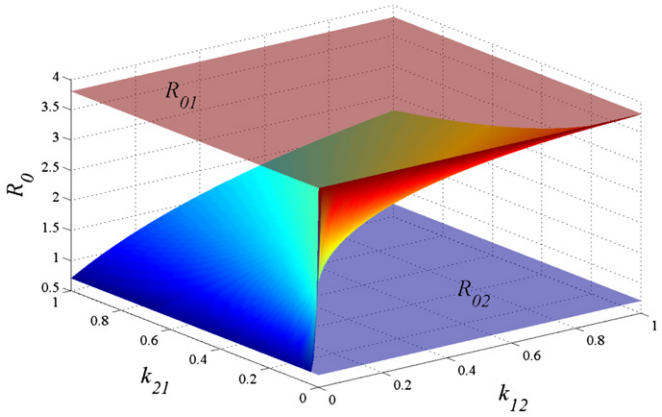

Fig. 2. R_0 plotted as a function of the migration rates k_{21} and k_{12}. The top and bottom planes represent R_{01} and R_{02}, respectively. In this graph, patch 1 is a high transmission patch, patch two is a low transmission patch, and conditions are dry in both patches ($R_{01} = 3.80$, $R_{02} = 0.70$).

As shown in Section 2.3, if the two patches have $R_{0i} > 1$, then the disease always persists. For example, suppose both patches are in the rainy season but patch one is a high-transmission patch and patch two is a low transmission patch so that $R_{01} = 187.15$ and $R_{02} = 7.03$. Then, we know that $7.03 \le R_0 \le 187.15$. Thus, it is clear in this scenario that no matter what the rate of migration is between the two patches, the disease will persist. Our numerical simulations of scenarios where both isolated patch reproduction numbers are greater than one (Fig. 3) suggest that migration causes the system to reach equilibrium sooner than if the two patches were isolated. Note that in each model simulation, we set the initial patch population sizes equal to the equilibrium patch population sizes so that each patch's population remains constant over time; that is $N_i(t) = N_i^*$ for all time $t > 0$.

If the two patches have $R_{0i} < 1$, then the disease always goes to extinction. This scenario is illustrated in Fig. 4 with two low-transmission, dry-condition patches with the same isolated patch reproduction numbers, $R_{01} = R_{02} = 0.70$. Without migration, the dynamics within each patch are identical. Under the influence of human movement the disease still goes extinct in both patches, however, the number of cases decreases more sharply in patch 1, since migration into this patch is five times faster than migration into patch 2.

If both patches are dry with patch 1 being the high-transmission patch and patch 2 the low-transmission patch, then $R_{01} = 3.80$ and $R_{02} = 0.7021$. The continuity of R_0 with respect to the migration parameters indicates that there exists a rate κ such that $\min(R_0) > 1$ for all $(k_{12},k_{21}) \in [0,\infty) \times [0,\kappa)$. In fact, if $\kappa < r_1(R_{01}-1)$, then $R_0 > 1$ for all $(k_{12},k_{21}) \in [0,\infty) \times [0,\kappa)$. Since $r_1 = 1/150$, $R_0 > 1$ if $(k_{12},k_{21}) \in [0,\infty) \times [0,0.0187)$. This example illustrates that although the disease would become extinct in patch 2 if the two patches were isolated, the presence of sufficiently slow migration from patch 1 to patch 2 in our two-patch model allows the disease to persist in both patches. This result is also demonstrated in Fig. 5, which plots the number of infected humans over time for this High-Dry/Low-Dry scenario. Fig. 5(a) shows that if the two patches are isolated, the disease dies out in patch 2 but persists in patch 1. However, if the two patches are connected by human movement (as in subfigure (b)), although the prevalence of malaria in patch 1 at steady state decreases, there is now persistence of the disease in both patches and the total prevalence is higher than when the patches are isolated. Conversely, Fig. 6 illustrates how simply changing the migration rates so that $k_{21} \gg k_{12}$ can bring the reproduction number below one, resulting in eventual extinction of the disease in both patches.

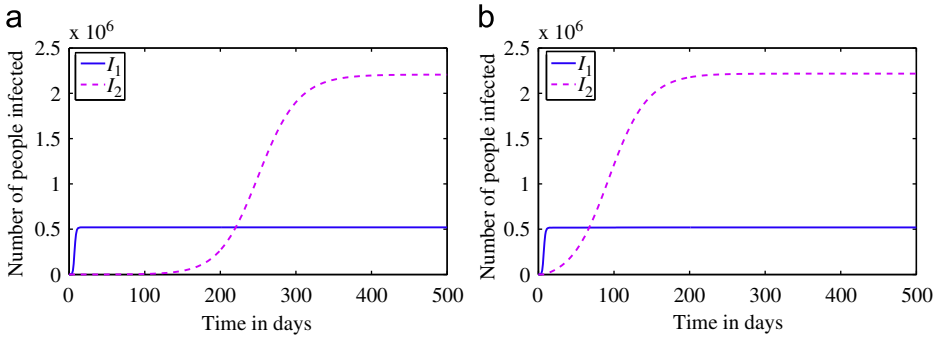

Fig. 3. Number of infected individuals in two wet condition patches. Patch 1 is high transmission ($R_{01} = 187.15$), patch 2 is low transmission ($R_{02} = 7.03$). (a) Patches are isolated, (b) patches are connected via human movement with migration rates $k_{12} = 0.001$, $k_{21} = 0.005$, resulting in $R_0 = 113.66$.

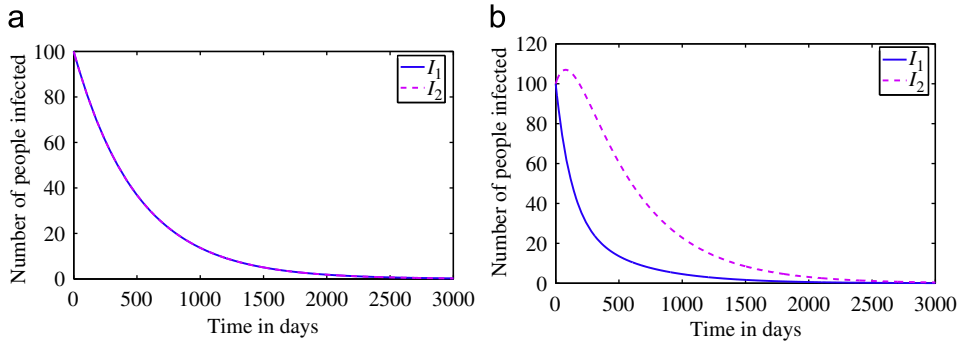

Fig. 4. Number of infected individuals in two low transmission, dry condition patches ($R_{01}=R_{02}=0.70$). (a) Patches are isolated, (b) patches are connected via human movement with migration rates $k_{12}=0.001$, $k_{21}=0.005$, resulting in R_0=0.70.

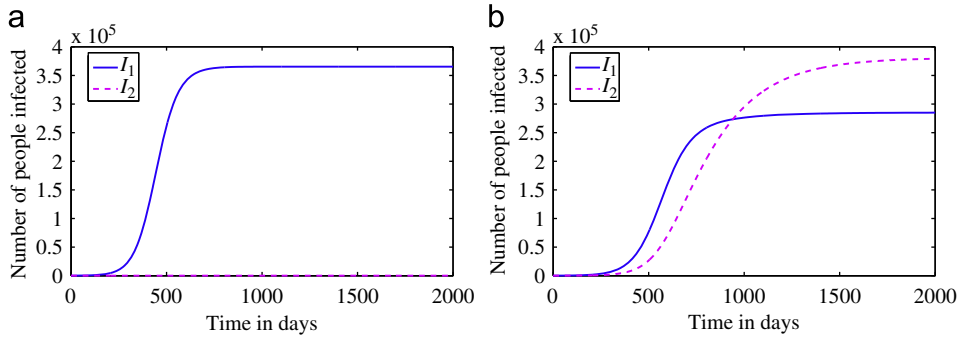

Fig. 5. Number of infected individuals in two dry condition patches. Patch 1 is high transmission ($R_{01}=3.80$), patch 2 is low transmission (R_{02}=0.70). (a) Patches are isolated, (b) patches are connected via human movement with migration rates $k_{12}=0.001$, $k_{21}=0.005$, resulting in R_0=2.35.

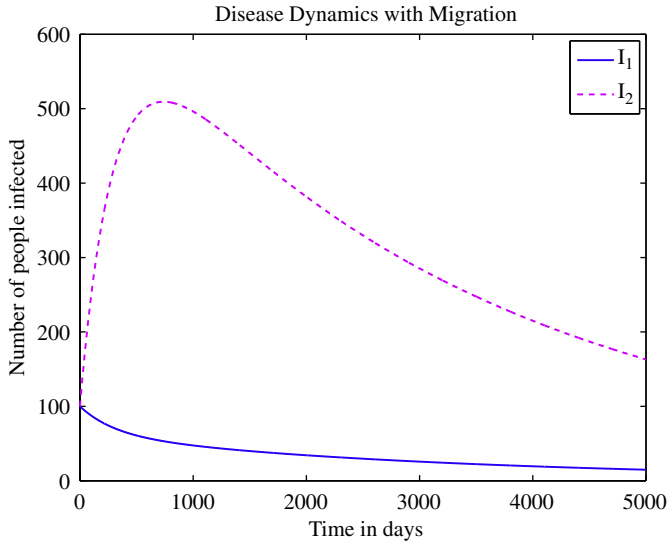

Fig. 6. Number of infected individuals in two dry condition patches. Patch conditions are identical to those in Fig. 5 with the exception of the migration rates. Patch 1 is high transmission ($R_{01}=3.80$), patch 2 is low transmission (R_{02}=0.70). Patches are connected via human movement with migration rates $k_{12}=0.0001$, $k_{21}=0.02$, resulting in R_0=0.99.

4.3. *Effect of migration on elasticity*

The elasticity of the global R_0 to most of a particular patch's parameters is entirely dependent upon two factors: the difference in the parameter values between the two patches, and migration. Similar to the effect of migration on R_0, the faster the movement from patch j to patch i is (in other words, the larger k_{ij} is), the more influence the parameters in patch i have on the system. For example, if a parameter, such as biting rate, has the same value in both patches, then the relative size of the migration rates and the relative values of R_{01} and R_{02} determine whether the basic reproductive number is more elastic to the parameter associated with patch 1 or the parameter associated with patch 2. On the other hand, if biting rate $a_1 > a_2$, ($k_{12}=k_{21}$), and ($R_{01}=R_{01}$), then the elasticity of R_0 to a_1 is larger than the elasticity of R_0 to a_2.

If $a_1 > a_2$, then if k_{21} is chosen appropriately and satisfies the inequality $k_{21} > k_{12}$ and R_{01} and R_{02} are not very different in value, then the elasticities related to these two parameters may become equal, or the elasticity of R_0 to a_1 may become smaller than the elasticity of R_0 to a_2. In other words, whether control measures should target patch 1 or patch 2 depends on the rate of human movement between the patches. In Section 3.2, we proved that $\varepsilon_{p_1}+\varepsilon_{p_2}$ is constant and equal to the elasticities in the isolated-patch case for $p_i=m_i,b_i,c_i$, and a_i. This result, which we demonstrate via numerical simulation in Fig. 7, suggests that it may be possible to divide resources, such as insecticide treated bed nets, between two connected patches in such a way that the control measures are as efficient as if the two patches were a single homogeneous patch. Still, numerical simulations are needed to identify which patch should be the primary target for malaria control.

Intuitively, we might choose to always target the higher transmission patch, however, our numerical simulations indicate that this is not always the best strategy for reducing malaria transmission. Fig. 7 illustrates, using the dry season parameterizations, how the elasticity of R_0 with respect to the model parameters changes for different rates of migration between a high transmission patch and a low transmission patch. In this example, $k_{12}=0.001$ and the elasticities are plotted as a function of k_{21}. For this High-Dry/Low-Dry scenario, if k_{21} is close to zero (i.e. no migration into patch 2), then any resources used to control malaria in the second patch will essentially be wasted. In particular,

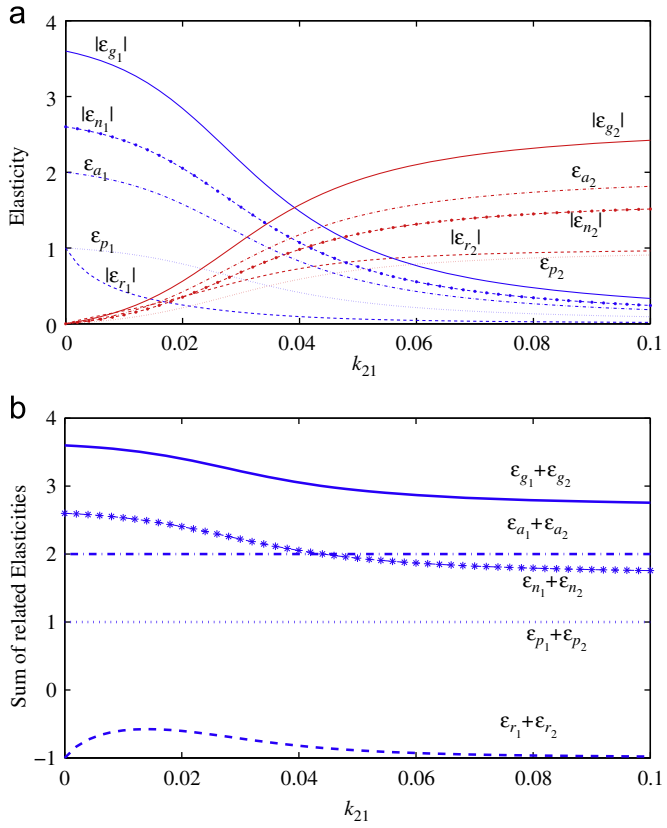

Fig. 7. (a) Elasticity of R_0 to all parameters, with $k_{12}=0.001$, plotted as functions of k_{21}. Patch 1 is a high transmission, dry conditions patch ($R_{01}=3.80$); patch 2 is a low transmission, dry conditions patch ($R_{02}=0.70$). Blue lines are elasticities with respect to patch 1 parameters; red lines are elasticities with respect to patch 2 parameters. (b) Sum of the elasticities ε_{p_1} and ε_{p_2} for each parameter p. (For interpretation of the references to color in this figure legend, the reader is referred to the web version of this article.)

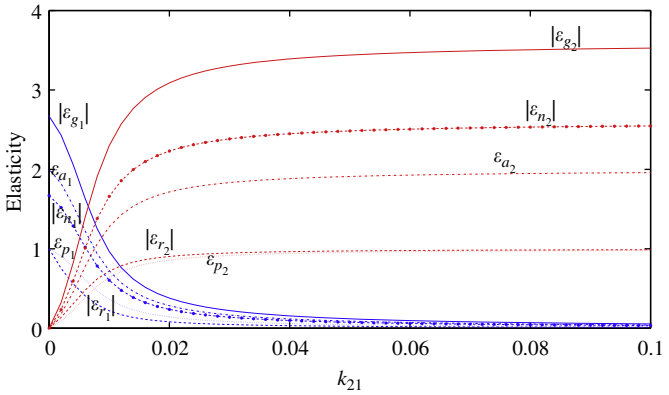

Fig. 8. Elasticity of R_0 to all parameters, with $k_{12}=0.001$, plotted as functions of k_{21}. Patch 1 is a low transmission, wet conditions patch ($R_{01}=7.03$); patch 2 is a high transmission, dry conditions patch ($R_{02}=3.80$). Blue lines are elasticities with respect to patch 1 parameters; red lines are elasticities with respect to patch 2 parameters. (For interpretation of the references to color in this figure legend, the reader is referred to the web version of this article.)

when k_{21} is small, R_0 is most elastic to mosquito death rate in patch 1 (g_1). As k_{21} is increased, R_0 becomes less sensitive to g_1 and eventually reaches a point where R_0 is equally elastic to g_1 and to g_2. Hence, at this intermediate k_{21} (approximately $k_{21}=0.04$), resources targeting mosquito death rate should be evenly divided between the two patches. If k_{21} increases further, R_0 is most sensitive to mosquito death rate in patch 2 (g_2). The elasticities with respect to parameters in patch 1 approach zero as k_{21} increases, suggesting that if migration into patch 2 is very fast, resources used for control in patch 1 will be wasted.

Because R_0 will be less than one for large enough k_{21} in the high-dry/low-dry scenario, the result that we should target the lower transmission patch when k_{21} exceeds a certain rate may not be surprising in a system where $R_{01}>1$ and $R_{02}<1$. However, a similar result holds even when both isolated-patch reproductive numbers are greater than one. Suppose, for example, that patch 1 has low-wet transmission characteristics and patch 2 has high-dry transmission characteristics so that $R_{01}>R_{02}>1$. The elasticities of R_0 to the model parameters are plotted in Fig. 8. As with the previous example where $R_{01}>1>R_{02}$, if migration into patch 2 is slow, control measures should target mosquito death rate in patch 1. However, if the migration rate k_{21} exceeds a certain value (approximately $k_{21}=0.007$), control efforts should target the patch with the lower reproductive number (patch 2).

Migration rates are often difficult to estimate. However, having an idea of the relative sizes of the migration parameters k_{12} and k_{21} might be sufficient to provide insight into where control measures should be implemented. In general, we found that in scenarios where $R_{01}>R_{02}>1$, or when $R_{01}>1>R_{02}$, control measures should target patch 2 if $k_{21}>>k_{12}$, and patch 1 should be targeted otherwise. Moreover, the larger k_{12} is, the smaller the ratio of k_{21} to k_{12} needs to be in order for patch 2 to be the more appropriate target for malaria control. For example, if patch 1 has low transmission, wet conditions and patch 2 has high transmission, dry conditions, so that $R_{01}>R_{02}>1$, then for $k_{12}=0.0001$, k_{21} must be more than 50 times greater than k_{12} in order for patch 2 to be the more important target for malaria control. If $k_{12}=0.001$, k_{21} need only be roughly 6.5 times greater than k_{12}, and if $k_{12}=0.01$, k_{21} must only be twice as big as k_{12} to warrant targeting patch 2. Consequently, being able to classify movement into the high transmission patch as either "fast" or "slow" provides additional insight into how resources for malaria control can be best allocated. In fact, if both migration rates are large and equal, then placing control measures in patch 1 will only be slightly more effective at reducing transmission than targeting patch 2 in the $R_{01}>R_{02}>1$ case, whereas if both migration rates are small and equal, targeting patch 1 should yield substantially better results than targeting patch 2. While decisions regarding where to allocate resources in the $R_{01}>1>R_{02}$ case follow the same general rules as in the $R_{01}>R_{02}>1$ case, the most significant qualitative difference between the two transmission scenarios occurs when both migration rates are large and equal: unlike with the $R_{01}>R_{02}>1$ case, patch 1 is a much better target for control than patch 2. We summarize these "rules of thumb" for where to target control measures in Tables 4 and 5.

Table 4
Target patch for malaria control in the $R_{01}>R_{02}>1$ case.

Ratio	k_{12} slow	k_{12} fast
$\frac{k_{21}}{k_{12}}\gg 1$	Patch 2	Patch 2
$\frac{k_{21}}{k_{12}}=1$	Patch 1	Patch 1 slightly better target
$\frac{k_{21}}{k_{12}}\ll 1$	Patch 1	Patch 1

Table 5
Target patch for malaria control in the $R_{01}>1>R_{02}$ case

Ratio	k_{12} slow	k_{12} fast
$\frac{k_{21}}{k_{12}}\gg 1$	Patch 2	Patch 2
$\frac{k_{21}}{k_{12}}=1$	Patch 1	Patch 1
$\frac{k_{21}}{k_{12}}\ll 1$	Patch 1	Patch 1

5. Elasticity analysis of endemic equilibrium

The elasticity analysis of the basic reproduction number provided insight into appropriate malaria interventions for reducing transmission intensity. We now turn to the study of the endemic equilibrium to determine whether the goal of reducing malaria prevalence requires a qualitatively different approach to malaria control.

Consider our equilibrium equation:

$$\frac{dI_i}{dt}=\frac{\alpha_i\beta_i I_i}{\beta_i I_i+g_i N_i}(N_i-I_i)-(r_i+k_{ji})I_i+k_{ij}I_j=0.$$

Multiplying throughout by $\beta_i I_i+g_i N_i$ yields

$$f_i(I_1,I_2):=\alpha_i\beta_i I_i(N_i-I_i)-(r_i+k_{ji})I_i(\beta_i I_i+g_i N_i)+k_{ij}I_j(\beta_i I_i+g_i N_i)=0. \quad (29)$$

We find the elasticity of the endemic equilibrium by differentiating system (29) implicitly, first with respect to the parameters α_i, β_i, r_i, g_i. From these elasticities, we can derive the elasticities for m_i and a_i since $\alpha_i=m_i a_i b_i e^{-g_i n_i}$ and $\beta_i=a_i c_i$. Implicit differentiation of $f_1(I_1^*,I_2^*)=0$ and $f_2(I_1^*,I_2^*)=0$ with respect to a parameter p_1 leads to the following system of two equations:

$$A_1\frac{\partial I_1^*}{\partial p_1}+B_1\frac{\partial I_2^*}{\partial p_1}+C_{p_1}=0, \quad (30)$$

$$B_2\frac{\partial I_1^*}{\partial p_1}+A_2\frac{\partial I_2^*}{\partial p_1}=0,$$

where

$$A_i=\alpha_i\beta_i(N_i^*-2I_i^*)-(r_i+k_{ji})(2\beta_i I_i^*+g_i N_i^*)+k_{ij}\beta_i I_j^*,$$

$$B_i=k_{ij}(\beta_i I_i^*+g_i N_i^*),$$

and

$$C_{\alpha_1}=\beta_1 I_1^*(N_1^*-I_1^*),$$

$$C_{\beta_1}=\alpha_1 I_1^*(N_1^*-I_1^*)+k_{12}I_1^*I_2^*-I_1^{*^2}(r_1+k_{21}),$$

$$C_{r_1}=-I_1^*(\beta_1 I_1^*+g_1 N_1^*),$$

$$C_{g_1}=-n_1\alpha_1\beta_1 I_1^*(N_1^*-I_1^*)-(r_1+k_{21})I_1^*N_1^*+k_{12}I_2^*N_1^*.$$

Proposition 5.0.1. $A_1A_2-B_1B_2\neq 0$. *Furthermore*, $A_1A_2-B_1B_2>0$.

Proof. From system (30), we have that

$$(A_1A_2-B_1B_2)\frac{\partial I_1^*}{\partial p_1}+C_{p_1}A_2=0. \quad (31)$$

Observe that $f_i(I_1,I_2)=A_iI_i+h_i$, where $h_i:=\alpha_i\beta_i I_i^2+(r_i+k_{ji})\beta_i I_i^2+k_{ij}I_j g_i N_i$ is strictly positive. Thus, $f(I_1^*,I_2^*)=0$ and $h_i^*,I_i^*>0$ imply that $A_i<0$.

Hence, Eq. (31) implies that $A_1A_2-B_1B_2$ and $\partial I_1^*/\partial p_1$ are nonzero as long as $C_{p_1}\neq 0$. Clearly $C_{\alpha_1}>0$ and $C_{r_1}<0$. We must verify that C_{β_1} and C_{g_1} are also nonzero.

Note that $f_i(I_1^*,I_2^*)=0$ implies

$$(r_i+k_{ji})I_i^*-k_{ij}I_j^*=\frac{\alpha_i\beta_i I_i^*}{\beta_i I_i^*+g_i N_i^*}(N_i^*-I_i^*)>0. \quad (32)$$

Using Eq. (32), we find that

$$C_{\beta_1}=\alpha_1 I_1^*(N_1^*-I_1^*)\left(1-\frac{\beta_1 I_1^*}{\beta_1 I_1^*+g_1 N_1^*}\right)>0,$$

$$C_{g_1}=-n_1\alpha_1\beta_1 I_1^*(N_1^*-I_1^*)-((r_1+k_{21})I_1^*-k_{12}I_2^*)N_1^*<0.$$

So, $C_{p_1}A_2\neq 0$ implies $A_1A_2-B_1B_2$ and $\partial I_1^*/\partial p_1$ are nonzero.

Now, $A_1A_2-B_1B_2$ nonzero and continuous in all parameters implies that it must have a definite sign: either strictly positive or strictly negative. Consider $k_{12}=k_{21}=0$. Then $A_1A_2-B_1B_2=A_1A_2>0$ implies that $A_1A_2-B_1B_2$ is strictly positive for all positive disease-related parameters and for all nonnegative migration rates k_{12}, k_{21}. □

Solving system (30) for the sensitivities $\partial I_1^*/\partial p_1$ and $\partial I_2^*/\partial p_1$ with $p_1=\alpha_1,\beta_1,r_1,g_1$, we have

$$\frac{\partial I_1^*}{\partial p_1}=-\frac{C_{p_1}A_2}{A_1A_2-B_1B_2}, \quad (33)$$

$$\frac{\partial I_2^*}{\partial p_1}=\frac{C_{p_1}B_2}{A_1A_2-B_1B_2}, \quad (34)$$

We obtained analogous equations for the sensitivities with respect to patch 2 parameters. The elasticity of I_i^* with respect to a parameter p_j is $\mathcal{E}_{p_j}^i=(p_j/I_i^*)(\partial I_i^*/\partial p_j)$ for $i,j\in\{1,2\}$. Moreover, the elasticity of the total malaria prevalence ($I^*=I_1^*+I_2^*$) with respect to parameter p_i is given by $\mathcal{E}_{p_i}=(I_1^*/(I_1^*+I_2^*))\mathcal{E}_{p_i}^1+(I_2^*/(I_1^*+I_2^*))\mathcal{E}_{p_i}^2$. From our analytic expressions, we can determine the sign of each elasticity. As we would expect, elasticities with respect to parameters m,a,b,c are positive and elasticities with respect to parameters r, g, and n are negative.

To visualize the elasticities, we first solve for the endemic equilibrium (I_1^*,I_2^*) numerically for a range of migration rates. Next, we substitute these values into our analytic expressions for the elasticities and, as we did for the elasticities of R_0, we plot the endemic equilibrium elasticities (in absolute value) as a function of k_{21}, with $k_{12}=0.001$ fixed (see Fig. 9).

Fig. 9(a) illustrates the elasticities of the endemic equilibrium in the High-Dry/Low-Dry setting, plotted for the range of migration rates for which the endemic equilibrium exists. For $k_{21}\geq 0.028$, $R_0<1$, and hence the disease-free equilibrium is the only equilibrium.

Fig. 9 reveals that studying the endemic equilibrium yields results that are qualitatively similar to those obtained in our study of R_0. In particular, the within patch rankings of elasticities for a given transmission setting are essentially the same in the analysis of R_0 and the analysis of the endemic equilibrium (EE). In the High-Dry/Low-Dry setting ($R_{01}>1>R_{02}$), the ordering of both the R_0 elasticities (Fig. 7(a)) and the EE elasticities (Fig. 9(a)) is $|\mathcal{E}_{g_1}|>|\mathcal{E}_{n_1}|>\mathcal{E}_{a_1}>\mathcal{E}_{p_1}$ for patch 1 parameters and $|\mathcal{E}_{g_2}|>\mathcal{E}_{a_2}>|\mathcal{E}_{n_2}|>\mathcal{E}_{p_2}$ for patch 2 parameters. We do not include $|\mathcal{E}_{r_2}|$ in this ordering because the position this elasticity takes in the ranking changes as the migration rate k_{21} changes. In the Low-Wet/High-Dry setting ($R_{01}>R_{02}>1$), the elasticities of the EE (Fig. 9) also retain the same ordering as the elasticities of R_0 (Fig. 8): $|\mathcal{E}_{g_1}|>\mathcal{E}_{a_1}>|\mathcal{E}_{n_1}|>\mathcal{E}_{p_1}>|\mathcal{E}_{r_1}|$ and $|\mathcal{E}_{g_2}|>|\mathcal{E}_{n_2}|>\mathcal{E}_{a_2}>|\mathcal{E}_{r_2}|>\mathcal{E}_{p_2}$.

The elasticities of the endemic equilibrium also retain some of the qualitative behavior as the elasticities of R_0 with respect to which patch is the better target for control. In the Low-Wet/High-Dry setting, for very small values of k_{21}, analysis of the EE reveals patch 1 is the better target for control; beyond a certain migration rate, patch 2 becomes the better target. Similarly, patch 1 is the best target for control in the High-Dry/Low-Dry setting. However, since the endemic equilibrium only exists for a constrained set of migration rates k_{21}, there is no migration rate for which patch 2 becomes the better target for control under this parameterization. Perhaps if R_{02} were larger, but still less than one, we might see that patch 2 does become a better target for control before the global reproduction number falls below one.

The differences between the analysis of the endemic equilibrium and the reproduction number are quantitative in nature. The most striking difference is the value of k_{21} for which we should switch from targeting patch 1 to targeting patch 2. This

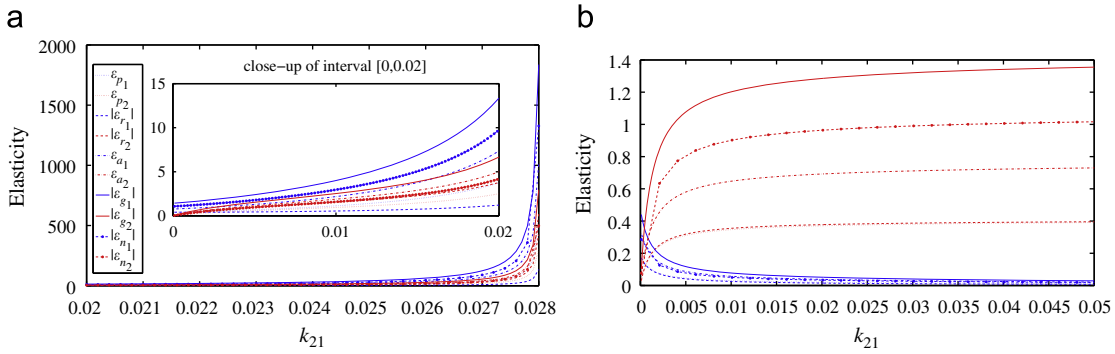

Fig. 9. Elasticity of endemic equilibrium to all parameters, with $k_{12}=0.001$, plotted as functions of k_{21}. Blue lines are elasticities with respect to patch 1 parameters; red lines are elasticities with respect to patch 2 parameters. (a) Patch 1 is a high transmission, dry conditions patch ($R_{01}=3.80$); patch 2 is a low transmission, dry conditions patch ($R_{02}=0.70$). Note that for $k_{21}\geq 0.028$, $R_0<1$. (b) Patch 1 is a low transmission, wet conditions patch ($R_{01}=7.03$); patch 2 is a high transmission, dry conditions patch ($R_{02}=3.80$). (For interpretation of the references to color in this figure legend, the reader is referred to the web version of this article.)

switch in strategy occurs for much smaller values of the migration rate k_{21} in our study of the EE than in our study of R_0. This indicates that determining an appropriate intervention strategy will depend, in part, on whether the goal is to reduce transmission potential or whether the goal is to reduce the overall prevalence of malaria. The qualitative similarities of within-patch elasticities, on the other hand, suggest that the best type of intervention (bed nets, treatment, insecticides, etc.) will be the same with either goal in mind.

6. Conclusion

Simple malaria models, such as the Ross–Macdonald model, that assume populations are isolated and homogeneous have made a large contribution to the area of malaria research over the last several decades. However, the diversity inherent to this disease requires models that incorporate heterogeneity so that they may provide greater insight into how we should approach malaria control. Our study of a two-patch malaria model suggests that using intuition to guide decision making in malaria control may not be sufficient. For example, targeting regions with the highest transmission rates may not be the most effective use of resources if they are strongly connected to lower transmission regions via emigration. Furthermore, using single-patch models to estimate parameters relevant to malaria dynamics and malaria control, such as the basic reproduction number, may provide an inaccurate assessment of transmission potential in a region. This discrepancy became clear in our exploration of the scenario where $R_{01}>1>R_{02}$. The two-patch malaria model indicates that human movement can result in the persistence of malaria in regions where malaria would die out if isolated, whereas a single-patch malaria model would inaccurately predict extinction of malaria in such situations.

Our results are similar to those found by Cosner et al. (2009), as our results also show that human movement can cause malaria to be endemic in an area with a reproduction number below 1. However, unlike Cosner's two-patch malaria model with Lagrangian movement, it is not possible for malaria to persist in our model if both regions have an isolated reproduction number below one. Whereas Cosner's exploration of a two-patch system assumes zero transmission in one patch, our results allow for an additional level of resolution. Because we assume each patch is capable of supporting malaria transmission, we are able to compare the elasticity of the global R_0 to reductions in transmission in both the high and low transmission patches. This allowed us to investigate how implementing control measures in different, but connected, regions impacts the overall level of transmission.

The results from our elasticity analysis of the two-patch model R_0 are also fundamentally different from elasticity analyses performed on single-patch malaria models. This is especially true for the parameters $1/g$ and n, which represent the mosquito lifespan and the extrinsic incubation period; many other models that have assessed elasticities did not include the extrinsic incubation period, and consequently reported biting rate a to be the most important parameter to target (Chitnis et al., 2008). In all four of our parameter sets, the average lifespan of a mosquito was shorter than the extrinsic incubation period. From our elasticity analysis, this implied that R_0 was more sensitive to mosquito death rate than to biting rate in all scenarios. We expect this relationship between mosquito lifespan and extrinsic incubation period to be true in the field under situations where less than half of the mosquito population that gets infected actually becomes infectious (Midega et al., 2007). This is not uncommon, as average daily survivorship of female mosquitoes ranges from 0.95 (Midega et al., 2007) to 0.68 (Rodriguez et al., 1992), yielding a probability of becoming infectious from 60% to under 2%, respectively, given a 10 day extrinsic period (White, 1982).

These results suggest that using multi-patch malaria models can help inform intervention strategy usage in areas of heterogeneous malaria transmission connected by human movement. For example, in Hispaniola, while conventional wisdom may suggest that resources should be focused on Haiti, which has higher malaria transmission, our results suggest this is not necessarily the case; efficient application of intervention strategies will depend also on human movement patterns between the two countries.

Comparing the endemic equilibrium elasticity results to the R_0 elasticity results suggests that it may be necessary to develop different control strategies depending on whether the goal is to reduce the transmission potential, or whether the goal is to reduce disease prevalence in a malaria endemic setting. Once a goal is established, knowledge about human migration rates will be essential to identifying an effective control strategy that makes efficient use of available resources.

Although this exploration of malaria dynamics and malaria control in the context of a two-patch model is still an oversimplification of reality, it highlights the need for more complex mathematical models incorporating both spatial heterogeneity and human movement to guide public health officials in the process of making decisions that will make the best use of the limited resources they have. Our study also stresses the importance of collecting malaria prevalence data and human movement

data in malaria endemic regions so that these more sophisticated models can provide reasonable, region-specific answers about how to best allocate resources.

Acknowledgments

We give special thanks to our QSE3 IGERT teammates Miguel Acevedo, Trevor Caughlin, and Kenny Lopiano for playing an active role in our weekly research discussions, and to Dr. Craig Osenberg for his guidance and support throughout this project.

This research was partially supported by the National Science Foundation under Grant No. 0801544 in the Quantitative Spatial Ecology, Evolution and Environment Program at the University of Florida.

References

Adler, F.R., 1993. Migration alone can produce persistence of host-parasitoid models. Am. Nat. 141 (4), 642–650.

Arino, J., van den Driessche, P., 2003. The basic reproduction number in a multi-city compartmental epidemic model. Lecture Notes in Control and Information Science, vol. 294; 2003, pp. 135–142.

Arino, J., van den Driessche, P., 2003. A multi-city epidemic model. Math. Popul. Stud. 10, 175–193.

Bailey, N.T.J., 1982. The Biomathematics of Malaria. Oxford University Press.

Beier, J.C., Davis, J.R., Vaughan, J.A., Noden, B.H., Beier, M.S., 1991. Quantitation of *Plasmodium falciparum* sporozoites transmitted in vitro by experimentally infected *Anopheles gambiae* and *Anopheles stephensi*. Am. J. Trop. Med. Hyg. 44 (5), 564–570.

Bekessy, A., Molineaux, L., Storey, J., 1976. Estimation of incidence and recovery rates of *Plasmodium falciparum* parasitaemia from longitudinal data. Bull. World Health Organ. 54, 685–693.

Bonnet, S., Gouagna, C., Safeukui, I., Meunier, J.-Y., Boudin, C., 2000. Comparison of artificial membrane feeding with direct skin feeding to estimate infectiousness of *Plasmodium falciparum* gametocyte carriers to mosquitoes. Trans. R. Soc. Trop. Med. Hyg. 94, 103–106.

CDC. Malaria facts. 〈http://www.CDC.gov/Malaria/about/facts.html〉.

Chitnis, N., Hyman, J., Cushing, J., 2008. Determining important parameters in the spread of malaria through the sensitivity analysis of a mathematical model. Bull. Math. Biol. 70, 1272–1296. doi:10.1007/s11538-008-9299-0.

Chiyaka, C., Mukandavire, Z., Das, P., Nyabadza, F., Hove-Musekwa, S.D., Mwambi, H., 2010. Theoretical analysis of mixed Plasmodium malariae and Plasmodium falciparum infections with partial cross-immunity. J. Theor. Biol. 263 (2), 169–178.

Collins, W.E., Jeffery, G.M., 2003. A retrospective examination of mosquito infection on humans infected with *Plasmodium falciparum*. Am. J. Trop. Med. Hyg. 68 (3), 366–371.

Collins, W.E., Warren, M., Skinner, J.C., Richardson, B.B., Kearse, T.S., 1977. Infectivity of the Santa Lucia (El Salvador) strain of *Plasmodium falciparum* to different Anophelines. J. Parasitol. 63 (1), 57–61.

Cosner, C., Beier, J.C., Cantrell, R.S., Impoinvil, D., Kapitanski, L., Potts, M.D., Troyo, A., Ruan, S., 2009. The effects of human movement on the persistence of vector-borne diseases. J. Theor. Biol. 258 (4), 550–560.

Costantini, C., Li, S.G., Torre, A.D., Sagnon, N., Coluzzi, M., Taylor, C.E., 1996. Density, survival and dispersal of *Anopheles gambiae* complex mosquitoes in a West African Sudan savanna village. Med. Vet. Entomol. 10 (3), 203–219.

Das, P., Horton, R., 2010. Malaria elimination: worthy, challenging, and just possible. The Lancet 376 (9752), 1515–1517.

deKroon, H., Plaisier, A., van Groenendael, J., Caswell, H., 1986. Elasticity: the relative contribution of demographic parameters to population growth rate. Ecology 67 (5), 1427–1431.

Diekmann, O., Heesterbeek, J.A.P., Metz, J.A.J., 1990. On the definition and the computation of the basic reproduction ratio R_0 in models for infectious diseases in heterogeneous populations. J. Math. Biol. 28, 365–382.

Fontenille, D., Lochouarn, L., Diagne, N., Sokhna, C., LeMasson, J., Diatta, M., Konate, L., Faye, F., Rogier, C., Trape, J., 1997. High annual and seasonal variations in malaria transmission by Anophelines and vector species composition in Dielmo, a holoendemic area in Senegal. Am. J. Trop. Med. Hyg. 56 (3), 247–253.

Githeko, A., Ayisi, J., Odada, P., Atieli, F., Ndenga, B., Githure, J., Yan, G., 2006. Topography and malaria transmission heterogeneity in western Kenya highlands: prospects for focal vector control. Malar. J. 5 (1), 107.

Graves, P.M., Burkot, T.R., J Saul, A., Hayes, R.J., Carter, R., 1990. Estimation of Anopheline survival rate, vectorial capacity and mosquito infection probability from malaria vector infection rates in villages near Madang, Papua New Guinea. J. Appl. Ecol. 27 (1), 134–147.

Greenwood, B., Mutabingwa, T., 2002. Malaria in 2002. Nature 415 (687), 670–672.

Guinovart, C., Navia, M.M., Tanner, M., Alonso, P.L., 2006. Malaria: burden of disease. Curr. Mol. Med. 6 (4), 137–140.

Harrington, L.C., Scott, T.W., Lerdthusnee, K., Coleman, R.C., Costero, A., Clark, G.G., Jones, J.J., Kitthawee, S., Kittayapong, P., Sithiprasasna R, R., Edman, J.D., 2005. Dispersal of the dengue vector *Aedes aegypti* within and between rural communities. Am. J. Trop. Med. Hyg. 72 (2), 209–220.

Hay, S.I., Guerra, C.A., Tatem, A.J., Atkinson, P.M., Snow, R.W., 2005. Urbanization, malaria transmission and disease burden in Africa. Nature 3, 81–90.

Heppel, S.S., Pfister, C.A., de Kroon, H., 2000. Elasticity analysis in population biology: methods and applications. Ecology 81, 605–606.

Hess, G.R., 1996. Linking extinction to connectivity and habitat destruction in metapopulation models. Am. Nat. 148 (1), 226–236.

Hethcote, H.W., 1976. Qualitative analyses of communicable disease models. Math. Biosci. 28 (3–4), 335–356.

Holt, R.D., 1985. Population dynamics in two-patch environments: some anomalous consequences of an optimal habitat distribution. Theor. Popul. Biol. 28 (2), 181–208.

Keating, J., Krogstad, D.J., Eisele, T.P., 2010. Malaria elimination on hispaniola. Lancet Infect. Dis. 10 (5), 291–293.

Koella, J.C., 1991. On the use of mathematical models of malaria transmission. Acta Trop. 49 (1), 1–25.

Kulkarni, M.A., Desrochers, R.E., Kerr, J.T., 2010. High resolution niche models of malaria vectors in northern Tanzania: a new capacity to predict malaria risk? PLoS One 5 (2), e9396.

Laxminarayan, R., 2004. Act now or later? economics of malaria resistance. Am. J. Trop. Med. Hyg. 71 (Suppl. 2), 187–195.

Lindsay, S.W., Wilkins, H.A., Zieler, H.A., Daly, R.J., Petrarca, V., Byass, P., 1991. Ability of *Anopheles gambiae* mosquitoes to transmit malaria during the dry and wet season in an area of irrigated rice cultivation in The Gambia. J. Trop. Med. Hyg. 94 (5), 313–324.

Loyola, E.G., Gonzalez-Ceron, L., Rodriguez, M.H., Arredondo-Jimenez, J.I., Bennett, S., Bown, D.N., 1993. *Anopheles albimanus* (Diptera: culicidae) host selection patterns in three ecological areas of the coastal plains of Chiapas, Southern Mexico. J. Med. Entomol. 30 (3), 518–523.

Machault, V., Vignolles, C., Pages, F., Gadiaga, L., Gaye, A., Sokhna, C., Trape, J.F., Lacaux, J.P., Rogier, C., 2010. Spatial heterogeneity and temporal evolution of malaria transmission risk in Dakar, Senegal, according to remotely sensed environmental data. Malar. J. 9 (1), 252.

Malaria Elimination Group. About the Malaria Elimination Group. 〈http://www.malariaeliminationgroup.org/about〉.

Martens, P., Hall, L., 2003. Malaria on the move: human population movement and malaria transmission. Emerg. Infect. Dis. 6 (2), 103–109.

Midega, J.T., Mbogo, C.M., Mwambi, H., Wilson, M.D., Ojwang, G., Mwangangi, J.M., Nzovu, J.G., Githure, J.I., Yan, G., Beier, J.C., 2007. Estimating dispersal and survival of *Anopheles gambiae* and *Anopheles funestus* along the Kenyan coast by using mark-release-recapture methods. J. Med. Entomol. 44 (6), 923–929.

Molineaux, L., Gramiccia, G., 1980. The Garki Project: Research on The Epidemiology and Control of Malaria in The Sudan Savanna of West Africa. WHO Publications, Albany, NY, USA.

Muir, L.E., Kay, B.H., 1998. *Aedes aegypti* survival and dispersal estimated by mark-release-recapture in northern Australia. Am. J. Trop. Med. Hyg. 58 (3), 277–282.

New York Times. December 2010. Comeback Against Malaria. 〈http://www.nytimes.com/2010/12/19/opinion/19sun2.html〉.

Ostfeld, R.S., Glass, G.E., Keesing, F., 2005. Spatial epidemiology: an emerging (or re-emerging) discipline. Trends Ecol. Evol. 20, 328–336.

Pickett, S.T.A., Cadenasso, M.L., 1995. Landscape ecology: spatial heterogeneity in ecological systems. Science 269 (5222), 15–20.

Prothero, R.M., 1977. Disease and mobility: a neglected factor in epidemiology. Int. J. Epidemiol. 6 (3), 259–267.

Robert, V., MacIntyre, K., Keating, J., Trape, J.F., Duchemin, J.B., Warren, M., Beier, J.C., 2003. Malaria transmission in urban sub-Saharan Africa. Am. J. Trop. Med. Hyg. 68 (2), 169–176.

Rodriguez, M.H., Bown, D.N., Arredondo-Jimenez, J.I., Villarreal, C., Loyola, E.G., Frederickson, C.E., 1992. Gonotrophic cycle and survivorship of *Anopheles albimanus* (Diptera: culicidae) in Southern Mexico. J. Med. Entomol. 29 (3), 395–399.

Russell, R.C., Webb, C.E., Williams, C.R., Ritchie, S.A., 2005. Mark-release-recapture study to measure dispersal of the mosquito *Aedes aegypti* in Cairns, Queensland, Australia. Med. Vet. Entomol. 19 (4), 451–457.

Sachs, J., Malaney, P., 2002. The economic and social burden of malaria. Nature 415, 680–685.

Salmani, M., van den Driessche, P., 2006. A model for disease transmission in a patchy environment. Discrete Continuous Dyn. Syst. Ser. B 6, 185–202.

Smith, D.L., McKenzie, E.F., 2004. Statics and dynamics of malaria infection in *Anopheles* mosquitoes. Malar. J. 3 (1), 13.

Smith, T., Charlwood, J.D., Kihonda, J., Mwankusye, S., Billingsley, P., Lyimo, E., Teuscher, T., Tanner, M., 1993. Absence of seasonal variation in malaria parasitaemia in an area of intense seasonal transmission. Acta Trop. 54, 55–72.

Stoddard, S.T., Morrison, A.C., Vazquez-Prokopec, G.M., Soldan, V.P., Kochel, T.J., Kitron, U., Elder, J.P., Scott, T.W., 2009. The role of human movement in the transmission of vector-borne pathogens. PLoS Neglected Trop. Dis. 3 (7), e481.

Tatem, A.J., Smith, D.L., 2010. International population movements and regional *Plasmodium falciparum* malaria elimination strategies. Proc. Natl. Acad. Sci. USA 107 (27), 12222–12227.

van den Driessche, P., Watmough, J., 2002. Reproduction numbers and subthreshold endemic equilibria for compartmental models of disease transmission. Math. Biosci. 180 (1–2), 29–48.
van Tienderen, P.H., 2000. Elasticities and the link between demographic and evolutionary dynamics. Ecology 81 (3), 666–679.
White, G.B., 1982. Malaria vector ecology and genetics. Br. Med. Bull. 38 (2), 207–212.
Woolhouse, M.E., Dye, C., Etard, J.F., Smith, T., Charlwood, J.D., 1997. Heterogeneities in the transmission of infectious agents: implications for the design of control programs. Proc. Natl. Acad. Sci. USA 94, 338–342.
World and Media, 2011. Malaria Scientists set Sights on Global Eradication. 〈http://www.worldandmedia.com/health/malaria-scientists-set-sights-on-global-eradication-1-0-3101.html〉.